

## Resonance Raman Study on Photoreduction of Iron-Porphyrins. A Novel Insight into the Ligand-Aided Process

Vlastimil FIDLER,<sup>††</sup> Takashi OGURA, Shin-ichiro SATO, Katsuhiko AOYAGI,<sup>†</sup> and Teizo KITAGAWA\*

Institute for Molecular Science, Okazaki National Research Institutes, Myodaiji, Okazaki 444

<sup>†</sup>Department of Industrial Chemistry, Fukushima National College of Technology, Taira, Iwaki, Fukushima 970  
(Received March 14, 1991)

Photoreduction of Fe(OEP) (OEP: octaethylporphyrin) in organic solvents by visible light was demonstrated to be a ligand-aided process in which simultaneous coordinations of a base such as 2-methylimidazole (2MeIm) and of an aliphatic alcohol to two axial positions of the iron ion were required. Coordination of an alcohol was evidenced from the observation of the Fe–alcohol stretching ( $\nu_{\text{Fe-alcohol}}$ ) resonance Raman (RR) band. Since this band exhibited an appreciable frequency shift between ROH and ROD, coordination of the alcohol in a protonated form was suggested. When a primary or secondary alcohol was added to the  $\text{CH}_2\text{Cl}_2$  solution of  $\text{Fe}^{\text{III}}$  (OEP)Cl in the presence of 2MeIm, a new absorption band appeared around 560–590 nm and the  $\nu_{\text{Fe-alcohol}}$  RR band was most intense for excitation at the maximum of the new absorption band. The new absorption was therefore assigned to the alcohol to  $\text{Fe}^{\text{III}}$  charge transfer (CT) band. A tertiary alcohol gave neither the CT band nor the  $\nu_{\text{Fe-alcohol}}$  RR band, although some spectral changes were noticed after long laser illumination at 441.6 nm, and the photoreduction as seen for other alcohol solutions did not take place. This photoreduction was not apparently recognized in the presence of oxygen. However, flash photolysis experiments demonstrated that the photoreduction occurs irrespective of the presence or absence of oxygen but rapid reoxidation results in apparent no effect.

Photoreduction of iron-porphyrins has been attracting chemists' interest since the initial finding of photoreduction on cytochrome oxidase by visible light.<sup>1–3)</sup> Afterwards the photoreduction has been extensively observed for various heme proteins<sup>4–8)</sup> and metalloporphyrins.<sup>9–16)</sup> While a mechanism of photoreduction of Pd-, Zn-, and a few water soluble porphyrins has been studied in detail,<sup>9,16)</sup> little is known about the photoreduction mechanism of iron porphyrins as well as heme proteins. Ozaki et al.<sup>17)</sup> recognized occurrence of photoreduction of an iron porphyrin during resonance Raman (RR) measurements of 2-methylimidazole (2MeIm) complex of  $\text{Fe}^{\text{III}}$ (OEP)Br in  $\text{CH}_2\text{Cl}_2$  (OEP: octaethylporphyrin). It was shown that any ring reduction to a porphyrin anion radical or chlorin did not take place and that the photoreduction was a ligand-aided process.

Recently, we noticed that the photoreduction observed by Ozaki et al.<sup>17)</sup> was catalyzed by a trace amount of alcohol contained as a stabilizer of solvent.<sup>18,19)</sup> In this paper we report detailed results on isotope substitution experiments which show that the catalytic alcohol binds to the sixth coordination position of  $\text{Fe}^{\text{III}}$ (OEP)(2MeIm) in the ROH form and gives rise to a charge transfer (CT) band around 560–590 nm. Although apparently the photoreduction does not seem to occur in the presence of oxygen, the flash photolysis experiments revealed that the photoreduction occurred but it was promptly reoxidized. It is most surprising that the laser illumination within the CT band induces no photoreduction.

### Experimental

$\text{Fe}^{\text{III}}$ (OEP)X (X=Cl, Br, and I) were synthesized by the procedure described elsewhere.<sup>20,21)</sup> Since no difference was observed by using X=Cl, Br or I for  $\text{Fe}^{\text{III}}$ (OEP)X,  $\text{Fe}^{\text{III}}$ (OEP)Cl was used unless otherwise stated. 2MeIm was recrystallized from benzene and its  $^1\text{H}$  NMR spectrum did not show any detectable impurity.  $\text{CH}_2\text{Cl}_2$  of spectroscopic grade from different suppliers were found to contain different stabilizers. We analyzed  $\text{CH}_2\text{Cl}_2$  from Wako, Kanto-kagaku, Cica-MERCK, Aldrich, and Dojin companies with gas chromatography and their influence on photoreduction of  $\text{Fe}^{\text{III}}$ (OEP)(2MeIm). Since the Cica-MERCK product contained the smallest amount of stabilizer and/or impurities (less than 0.1%) and had no side-effect on photoreduction, it was used without further purification. The standard concentration of the sample was 2 mM of  $\text{Fe}^{\text{III}}$ (OEP)X, 50–100 mM of 2MeIm, and a few % (v/v) of added alcohol. Fresh solution was prepared for each experiment.

Raman spectra were measured with a JEOL-400D Raman spectrometer equipped with a cooled RCA-31034a photomultiplier and a home-made computer-controlled data acquisition system based on NEC 9801 computer. As an excitation source of Raman scattering were used  $\text{Kr}^+$  laser (Spectra Physics, 164), He/Cd laser (Kinmon Electronics, CDR80MGE),  $\text{Ar}^+$  laser (NEC, GLG3200), and  $\text{Ar}^+$  laser-pumped dye laser (Spectra Physics, 164/175) with rhodamine 6G. Laser power was measured at the sample point with a hand power-meter (Advantest TA-8210). Raman shifts were calibrated with indene for individual excitation lines. Uncertainties in wave-numbers of well-defined band are less than  $\pm 1 \text{ cm}^{-1}$ . During the Raman measurements the sample was kept at  $10^\circ\text{C}$  by circulating temperature-controlled water through the cell holder. For the measurements under anaerobic conditions, the sample solution in the air-tight cell was degassed through three freeze/thaw cycles and stopped by a cock.

Conventional absorption spectra were recorded with a Hitachi 220S spectrophotometer. For the test of photoreduc-

<sup>††</sup> Present address: Department of Physical Chemistry, Faculty of Science, Charles University, 128-40 Praha 2, Czechoslovakia.

tion the sample in the anaerobic cell was illuminated by a projector lamp through the short cut filter (L-38, Hoya Corp.) for 5 min. During illumination the sample cell was placed in a water bath at 20 °C. Time profiles of absorption changes of the sample after pulse illumination were measured by a home-made apparatus described elsewhere.<sup>22)</sup>

### Results

At the beginning of this study we encountered some problems regarding reproducibility of the previous results.<sup>17)</sup> The RR spectrum of  $\text{Fe}^{\text{III}}(\text{OEP})(2\text{MeIm})$  (Fig. 1A) was the same as that reported previously<sup>17)</sup> but  $\text{Fe}^{\text{III}}(\text{OEP})(2\text{MeIm})$  in pure  $\text{CH}_2\text{Cl}_2$  did not exhibit any photoreduction even after careful degassing and long-lasting illumination by white light or laser. Figure 1(B) shows the spectrum obtained for  $\text{Fe}^{\text{III}}(\text{OEP})\text{Cl}$  in a  $\text{CH}_2\text{Cl}_2$ - $\text{CH}_3\text{OH}$  mixed solvent (1:1 in v/v). This is again the same as that of  $\text{Fe}^{\text{III}}(\text{OEP})\text{Cl}$ . Following systematic tests of all components of the system revealed that photoreduction of  $\text{Fe}^{\text{III}}(\text{OEP})(2\text{MeIm})$  went on only when the solvent  $\text{CH}_2\text{Cl}_2$  contained alcohol as a stabilizer. Figure 1(C) shows the RR spectrum

observed for  $\text{Fe}^{\text{III}}(\text{OEP})(2\text{MeIm})$  in  $\text{CH}_2\text{Cl}_2$  in the presence of MeOH. The resultant spectrum remained unaltered by the concentration change of MeOH from 0.5 to 20% (v/v) and is the same as that of  $\text{Fe}^{\text{II}}(\text{OEP})(2\text{MeIm})$  as noted previously.<sup>17)</sup> In the presence of oxygen, however, the spectrum was the same as Fig. 1(A). It became evident, therefore, that both 2MeIm and MeOH are required for photoreduction to occur and apparently the photoreduction seems not to occur in the presence of oxygen. A similar phenomenon was seen for  $\text{Fe}^{\text{III}}(\text{OEP})(1,2\text{-Me}_2\text{Im})$  but not at all for  $\text{Fe}^{\text{III}}(\text{OEP})(\text{Im})_2$  and  $\text{Fe}^{\text{III}}(\text{OEP})(1\text{MeIm})_2$ .

Figure 2 shows the effect of alcohol on absorption spectra. The spectra in the upper panel were obtained in the presence of oxygen. Although Soret band is little affected by the presence of alcohol except its slight weakening, Q band of  $\text{Fe}^{\text{III}}(\text{OEP})(2\text{MeIm})$  at 535 nm disappears and a new band appears at 584 nm in the presence of MeOH (B). The 584 nm band did not appear when MeOH was added to  $\text{Fe}^{\text{III}}(\text{OEP})\text{Cl}$  in  $\text{CH}_2\text{Cl}_2$ . A similar spectral change was observed when ethanol (EtOH), or 1-propanol (*n*-PrOH) was used for

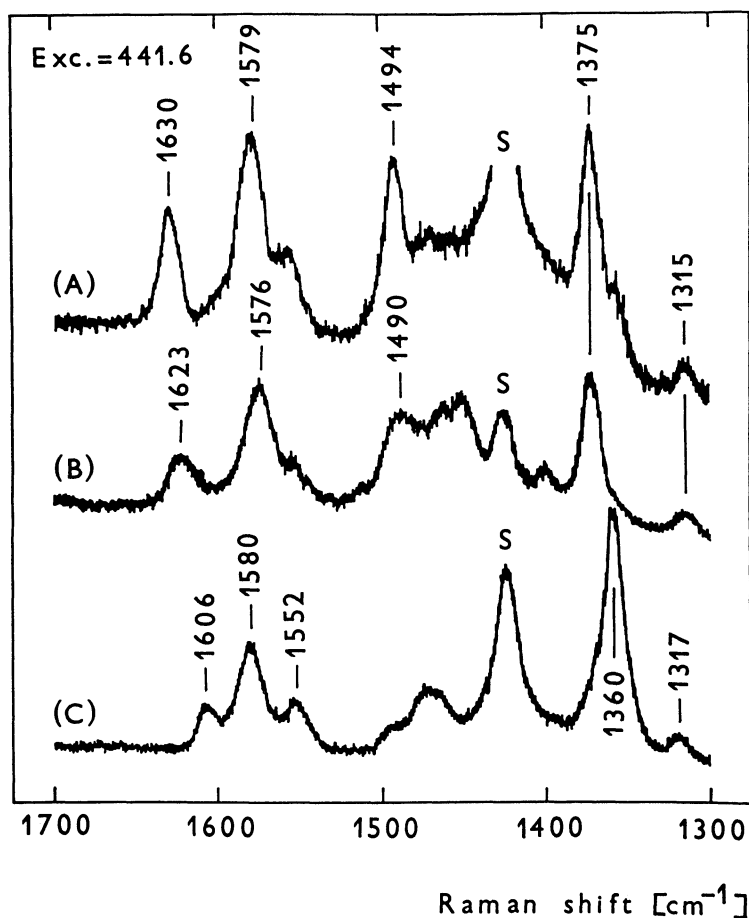


Fig. 1. Typical RR spectra of  $\text{Fe}(\text{OEP})$  complexes under different solvent conditions. A)  $\text{Fe}^{\text{III}}(\text{OEP})(2\text{MeIm})$  in  $\text{CH}_2\text{Cl}_2$ , B)  $\text{Fe}^{\text{III}}(\text{OEP})\text{Cl}$  in  $\text{MeOH}:\text{CH}_2\text{Cl}_2=1:1$  (v/v), C)  $\text{Fe}^{\text{III}}(\text{OEP})(2\text{MeIm})(\text{MeOH})$  in  $\text{CH}_2\text{Cl}_2$ . Excitation: 441.6 nm. All spectra were observed under anaerobic conditions.

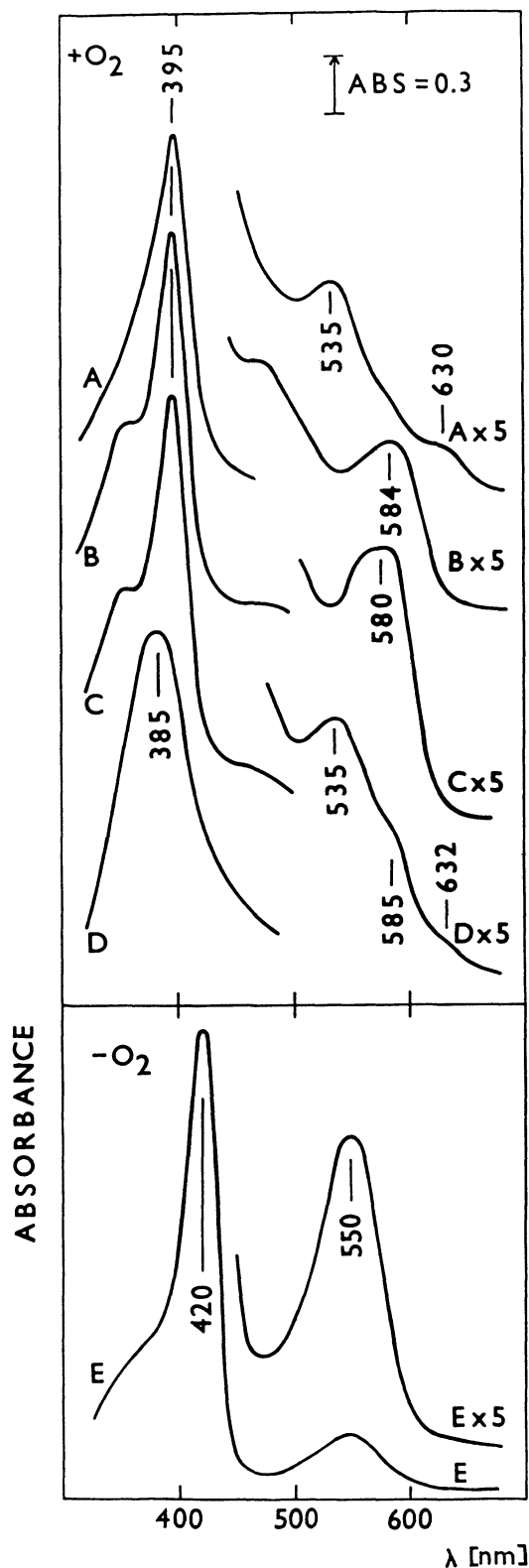


Fig. 2. Visible absorption spectra of  $\text{Fe}^{\text{III}}(\text{OEP})(2\text{MeIm})$  in various alcohol-containing  $\text{CH}_2\text{Cl}_2$  solutions. A) without alcohol, B) MeOH (EtOH and *n*-PrOH are the same as this), C) *i*-PrOH, D) *t*-BuOH, E) MeOH (EtOH, *n*-PrOH, and *i*-PrOH are the same as this). Spectra A through D (upper panel) were obtained in the presence of oxygen but spectrum E (lower panel) was obtained under anaerobic conditions.

$\text{Fe}^{\text{III}}(\text{OEP})(2\text{MeIm})$  (Fig. 2B). In the case of 2-propanol (*i*-PrOH) the new band was appreciably broader at 580 nm (Fig. 2C). A spectral change recognized for *t*-butyl alcohol (*t*-BuOH) was quite small in the 500–600 nm region as shown by Fig. 2D, but the shape of the Soret band was altered. When these solutions were brought to anaerobic conditions and subjected to light illumination at 380–450 nm, the spectrum shown in the lower panel (Fig. 2E) was obtained. It gave strong Soret band at 420 nm and weak Q band at 550 nm and the whole spectrum was almost the same as that of  $\text{Fe}^{\text{II}}(\text{OEP})(2\text{MeIm})$  prepared separately. Note that MeOH, EtOH, *n*-PrOH, or *i*-PrOH did not yield any difference in the resultant absorption spectra but *t*-BuOH did not induce the light-illumination effect. With this it changed only after long illumination of laser light at 441.6 nm; bands at 635 and 535 nm became pronounced and the Soret band shifted to red by a few nm. Consequently, it became evident that alcohols active to photoreduction cause a distinctive spectral change in the oxidized state, implying their coordination to the iron ion, but different alcohols bring no difference after photoreduction.

Since the active alcohols yield a new absorption band around 584–590 nm, RR spectra were excited at 590 nm. In contrast with the excitation at 441.6 nm, the RR spectra excited at 590 nm obtained in the absence of oxygen were the same as those obtained when it was present. The polarized RR spectra of  $\text{Fe}^{\text{III}}(\text{OEP})(2\text{MeIm})(\text{MeOH})$  and its *meso*-(5, 10, 15, 20-) deuterated and  $^{15}\text{N}$ -substituted derivatives are shown in Fig. 3 (1700–1300  $\text{cm}^{-1}$ ) and Fig. 4 (1300–900  $\text{cm}^{-1}$ ). The  $\nu_4$  band, which exhibits a downward shift by 6  $\text{cm}^{-1}$  upon  $^{15}\text{N}$ -substitution, appears at a typical frequency of iron(III) porphyrins (1376  $\text{cm}^{-1}$ ). Two anomalously polarized (ap) bands are seen at 1564 and 1315  $\text{cm}^{-1}$  which are little shifted upon  $^{15}\text{N}$ -substitution but greatly upon *meso*-deuteration; they are assigned to  $\nu_{19}$  and  $\nu_{21}$ , respectively.<sup>23–25</sup> The strong enhancement of the two ap bands is general characteristic of the Q-band excited RR spectra of metalloporphyrins.<sup>26,27</sup>

The highest frequency depolarized (dp) band, which exhibits a downshift by 16  $\text{cm}^{-1}$  upon *meso*-deuteration and 5  $\text{cm}^{-1}$  upon  $^{15}\text{N}$ -substitution, is assigned to  $\nu_{10}$ .<sup>23–25</sup> This band is sensitive to the coordination number;<sup>28,29</sup> in typical cases the five coordinate iron(III) high-spin complexes give it around 1629–1631  $\text{cm}^{-1}$  while the six-coordinate iron(III) high-spin complexes do it around 1615–1625  $\text{cm}^{-1}$ . Since  $\text{Fe}^{\text{III}}(\text{OEP})(\text{CH}_3\text{OH})_2$  and  $\text{Fe}^{\text{III}}(\text{OEP})(\text{Im})_2$  give  $\nu_{10}$  at 1624 and 1640  $\text{cm}^{-1}$ , respectively,<sup>30</sup> the present compounds are clearly different. For six-coordinate complexes with an oxygen of  $\text{ClO}_4^-$  and a nitrogen of pyridine derivative, which have the intermediate spin state,<sup>28</sup> this band is observed around 1634–1636  $\text{cm}^{-1}$ . Therefore, the  $\nu_{10}$  frequency is not unreasonable if the present compound is a six-coordinate intermediate spin complex. Its difference from the five-coordinate high-spin state is seen in the

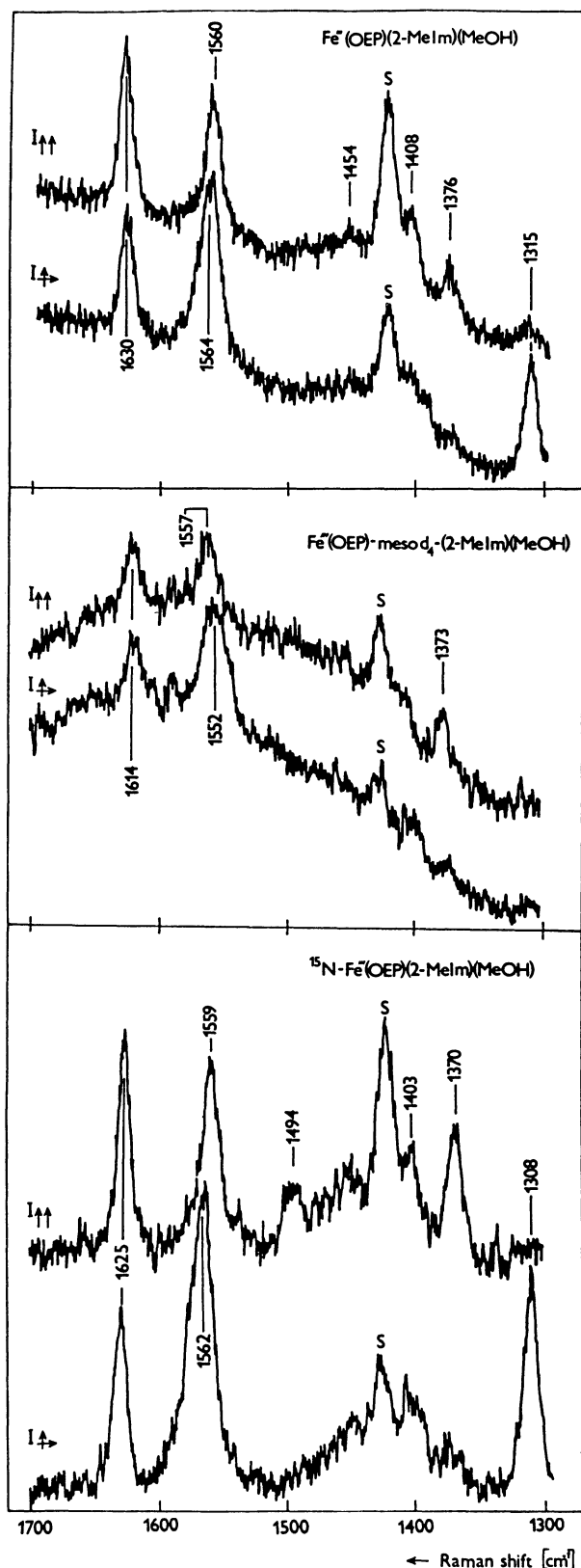


Fig. 3. Polarized RR spectra of  $\text{Fe}^{\text{III}}(\text{OEP})(2\text{MeIm})(\text{MeOH})$  (MeOH) and its isotopic substitutes in the 1700–1300  $\text{cm}^{-1}$  region;  $\text{Fe}^{\text{III}}(\text{OEP}-d_4)(2\text{MeIm})(\text{MeOH})$  (middle) and  $\text{Fe}^{\text{III}}(\text{OEP}-^{15}\text{N}_4)(2\text{MeIm})(\text{MeOH})$  (bottom). All spectra were excited at 590 nm (100 mW) under aerobic conditions.  $I_{||}$  and  $I_{\perp}$  mean the parallel and perpendicular components, respectively.

size of deuteration shift;  $^{15}\text{N}$ -isotope shift is much smaller (1  $\text{cm}^{-1}$ ) for five-coordinate complex<sup>31)</sup> than for the present complex (5  $\text{cm}^{-1}$ ).

In Figure 4 an ap band is observed at 1132  $\text{cm}^{-1}$  and is

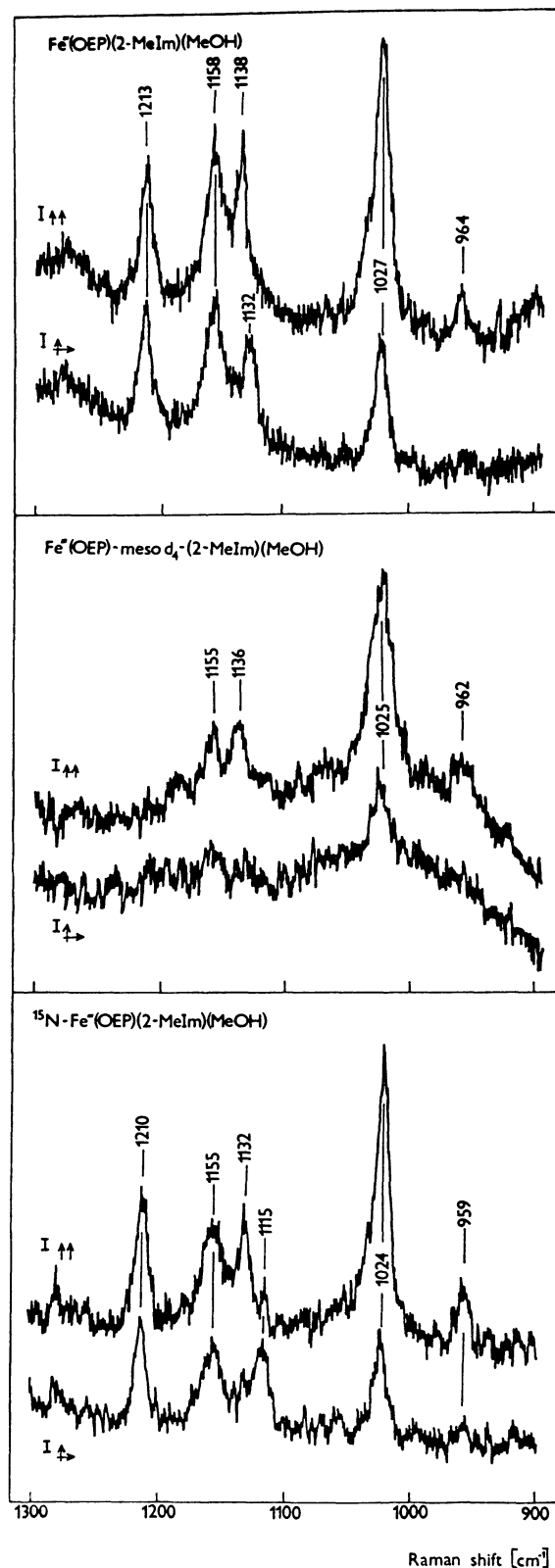


Fig. 4. The same set of spectra as in Fig. 3 but in the 1300–900  $\text{cm}^{-1}$  region.

assigned to  $\nu_{22}$ . This band is downshifted by  $17\text{ cm}^{-1}$  upon  $^{15}\text{N}$ -substitution for expectation of  $13\text{ cm}^{-1}$ ,<sup>24)</sup> and is thought to largely upshift to ca.  $1200\text{ cm}^{-1}$  upon *meso*-deuteration. Two p bands at  $1138$  and  $1027\text{ cm}^{-1}$  were originally assigned to a combination and  $\nu_5$  modes, respectively,<sup>24)</sup> but recently Li et al.<sup>25)</sup> reassigned them to  $\nu_5$  and the ethyl C–C stretching vibrations. Two dp bands at  $1213$  and  $1158\text{ cm}^{-1}$  are assigned to  $\nu_{13}$  and  $\nu_{30}$ ;  $\nu_{13}$  is expected to show little shift upon  $^{15}\text{N}$ -substitution but a large down-shift (to ca.  $950\text{ cm}^{-1}$ ) upon *meso*-deuteration, while  $\nu_{30}$  is expected to show little shift upon *meso*-deuteration and appreciable down-shift ( $9\text{--}10\text{ cm}^{-1}$ ) upon  $^{15}\text{N}$ -substitution.<sup>24,25)</sup>

The observed frequencies and isotope shifts of the alcohol complex are compared with those of  $\text{Fe}^{\text{III}}(\text{OEP})(2\text{MeIm})$  and  $\text{Fe}^{\text{III}}(\text{OEP})\text{Cl}$ <sup>31,32)</sup> in Table 1. The  $\nu_2$ ,  $\nu_{21}$ , and  $\nu_{22}$  frequencies are lower and the size of *meso*-deuteration shift of  $\nu_{19}$  is distinctly larger for  $\text{Fe}^{\text{III}}(\text{OEP})\text{Cl}$ . Therefore, even within the five coordinate ferric high-spin complexes,  $\text{Fe}^{\text{III}}(\text{OEP})(2\text{MeIm})$  is slightly different from  $\text{Fe}^{\text{III}}(\text{OEP})\text{Cl}$ . The magnitude of the isotopic frequency shifts reflects the vibrational displacement of the isotope-replaced atoms in the vibration in question and accordingly it is sensitive to the vibrational mode. On the basis of the observed isotopic shifts, the vibrational modes of  $\text{Fe}^{\text{III}}(\text{OEP})(2\text{MeIm})(\text{MeOH})$  are closer to those of  $\text{Fe}^{\text{III}}(\text{OEP})(2\text{MeIm})$  than to those of  $\text{Fe}^{\text{III}}(\text{OEP})\text{Cl}$ . It may imply the similarity of their geometrical structure and raise a question about the coordination of MeOH to the sixth coordination position.

The evidence for alcohol coordination was obtained from the  $590\text{ nm}$ -excited RR spectra in the lower frequency region shown in Figure 5. In the absence of MeOH, there are no prominent RR bands in the  $600\text{--}400\text{ cm}^{-1}$  region as shown by spectrum E. When  $\text{CH}_3\text{OH}$  was added to the  $\text{CH}_2\text{Cl}_2$  solution of  $\text{Fe}^{\text{III}}(\text{OEP})(2\text{MeIm})$ , a new band appeared at  $524\text{ cm}^{-1}$  as shown by spectrum B and it is shifted to a higher

frequency by  $4\text{ cm}^{-1}$  upon replacement of  $^{56}\text{Fe}$  with  $^{54}\text{Fe}$  as shown by spectrum A. Isotope replacement of  $\text{CH}_3\text{OH}$  with  $\text{CH}_3\text{OD}$  and  $\text{CD}_3\text{OD}$  gave rise to spectra C and D, respectively. The peak frequencies for  $\text{CH}_3\text{OH}$  and  $\text{CH}_3\text{OD}$  derivatives are definitely different, indicating that MeOH is bound in the protonated form but not in the alkoxide form. When we assume that MeOH is a single dynamic unit, a simple harmonic approximation for the Fe–MeOH stretching vibration provides the isotopic frequency shifts as follows;  $+3.5\text{ cm}^{-1}$  for  $^{54}\text{Fe}$ ,  $-5.0\text{ cm}^{-1}$  for  $\text{CH}_3\text{OD}$ , and  $-18.7\text{ cm}^{-1}$  for  $\text{CD}_3\text{OD}$ . The observed value for  $^{54}\text{Fe}$  agrees with the expected one but those for MeOH are smaller than expected values, implying the vibrational coupling of the Fe–alcohol stretching mode with internal vibrations of MeOH. Anyway, the  $524\text{ cm}^{-1}$  band is assigned to the Fe–MeOH stretching vibration. This band did not appear in the  $\text{MeOH-CH}_2\text{Cl}_2$  (1 : 1 in v/v) mixed solution of  $\text{Fe}^{\text{III}}(\text{OEP})\text{Cl}$ . It means that the  $524\text{ cm}^{-1}$  band appears from the six-coordinated complex with MeOH and 2MeIm as axial ligands.

The excitation profile of the  $524\text{ cm}^{-1}$  band is illustrated in Fig. 6, where relative intensities of the  $524\text{ cm}^{-1}$  band to the solvent band at  $1158\text{ cm}^{-1}$  are plotted against the excitation wavelengths. The relative intensities were corrected for different transmittances at  $524$  and  $1158\text{ cm}^{-1}$  for each excitation wavelength on the basis of the observed transmission spectrum. The broken line in Fig. 6 indicates the background subtracted absorption spectrum for the  $585\text{-nm}$  band which is normalized at the maximum absorption to the Raman excitation profile. The peak of Raman excitation profile is noticeably coincident with the absorption curve, suggesting strongly that the  $585\text{ nm}$  absorption has a charge transfer character from MeOH to the  $\text{Fe}^{\text{III}}$  ion.

The Raman excitation at  $585\text{ nm}$  within the CT band did not exhibit a trace of Raman spectrum of the reduced species; this was unexpected. This is not due to poor resonance but to nonphotoreduction. Indeed,

Table 1. Comparison of the Observed Frequencies and Isotopic Frequency Shifts of  $\text{Fe}^{\text{III}}(\text{OEP})(2\text{MeIm})(\text{MeOH})$  with Those of  $\text{Fe}^{\text{III}}(\text{OEP})(2\text{MeIm})$  and  $\text{Fe}^{\text{III}}(\text{OEP})\text{Cl}$

Mode	P <sup>a)</sup>	$\text{Fe}^{\text{III}}(\text{OEP})(2\text{MeIm})(\text{MeOH})$			$\text{Fe}^{\text{III}}(\text{OEP})(2\text{MeIm})$			$\text{Fe}^{\text{III}}(\text{OEP})\text{Cl}$		
		$\nu$	$\Delta\nu(^{15}\text{N})^{\text{b)}}$	$\Delta\nu(\text{D})^{\text{c)}}$	$\nu$	$\Delta\nu(^{15}\text{N})$	$\Delta\nu(\text{D})$	$\nu$	$\Delta\nu(^{15}\text{N})^{\text{d)}}$	$\Delta\nu(\text{D})^{\text{e)}}$
$\nu_{10}$	dp	1630	–5	–16	1629	–1	–13	1629	–1	–12
$\nu_{19}$	ap	1564	–2	–12	1564	+1	–8	1568	–1	–21
$\nu_2$	p	1560	–1	–3	1559	+2	0	1582	–1	–1
$\nu_{29}$	dp	1408	–5					1405	–1	–2
$\nu_4$	p	1376	–6	–3				1374	–5	–1
$\nu_{21}$	ap	1315	–7		1315	–5		1306	–2	
$\nu_{13}$	dp	1213	–3		1218	+3		1210	0	
$\nu_5$	p	1138	–6	–2				1135	–3	+1
$\nu_{22}$	ap	1132	–17					1125	–17	
$\text{C}_1\text{--C}_2$	p	1027	–3	–2	1025	0	0	1025	–1	+2
		964	–5	–2				964	–4	+3

a) Polarization property; p, polarized, dp, depolarized; ap, anomalously polarized. b) Isotopic shift upon  $^{15}\text{N}$ -substitution. c) Isotopic shift upon *meso*-deuteration. d) From Ref.18. e) From Ref. 19.

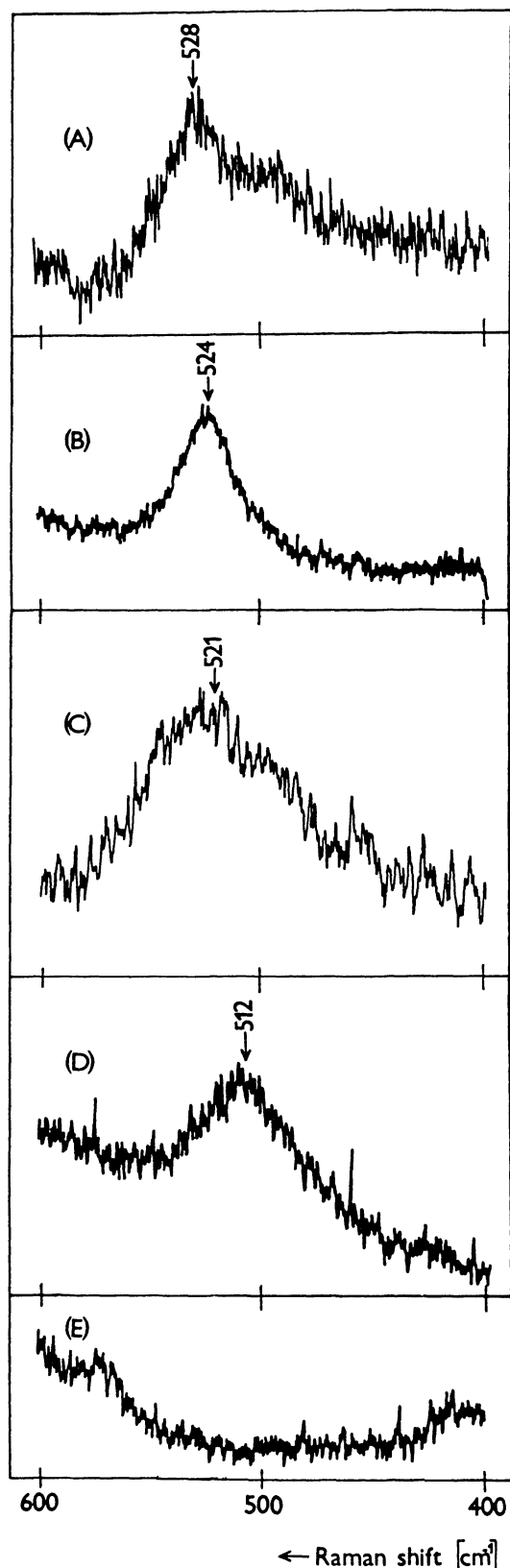


Fig. 5. Dependence of the  $524\text{ cm}^{-1}$  RR band on isotopic substitutions. A)  $^{54}\text{Fe}(\text{OEP})(2\text{MeIm})(\text{CH}_3\text{OH})$ , B)  $\text{Fe}^{\text{III}}(\text{OEP})(2\text{MeIm})(\text{CH}_3\text{OH})$ , C)  $\text{Fe}^{\text{III}}(\text{OEP})(2\text{MeIm})(\text{CH}_3\text{OD})$ , D)  $\text{Fe}^{\text{III}}(\text{OEP})(2\text{MeIm})(\text{CD}_3\text{OD})$ , E)  $\text{Fe}^{\text{III}}(\text{OEP})(2\text{MeIm})$  without methanol. All spectra were obtained with the 590 nm excitation line (100 mW) under aerobic conditions.

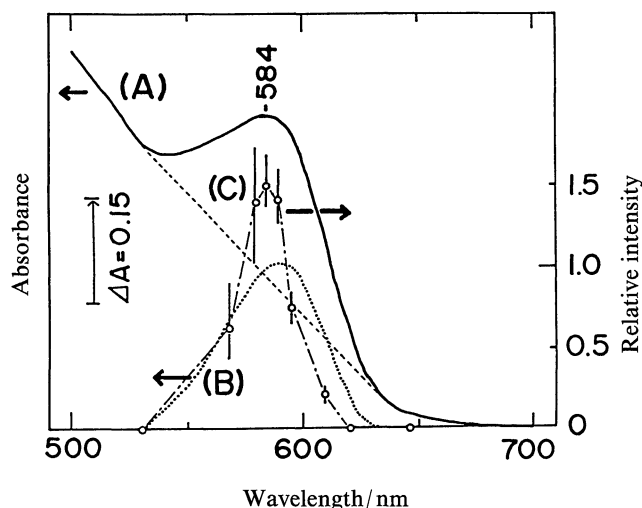


Fig. 6. Comparison of the excitation profile of the  $524\text{ cm}^{-1}$  RR band of  $\text{Fe}^{\text{III}}(\text{OEP})(2\text{MeIm})(\text{MeOH})$  with the absorption profile of the new band. A) Observed absorption curve, B) Approximate absorption profile of the new band that was obtained by subtracting an extrapolated tail (indicated by a broken line) of absorption from curve (A). The ordinate scale is illustrated by an arrow. C) Excitation profile of the  $524\text{ cm}^{-1}$  RR band represented in terms of its relative intensity to the solvent band at  $1158\text{ cm}^{-1}$ .

the anaerobic sample illuminated by laser light around 570–610 nm did not yield a change of visible absorption spectrum. Therefore, the mechanism of the photoreduction of  $\text{Fe}^{\text{III}}(\text{OEP})(2\text{MeIm})(\text{MeOH})$  is distinct from a trivial photoreduction in which the electron transfer takes place via a CT excited state.

Since no photoreduction was observed by a Raman spectrum in the presence of oxygen, we pursued the time course of the phenomenon by using transient absorption spectroscopy. The results are shown in Fig. 7(A), where a change of absorption at 420 nm is drawn against time; (a) and (b) were obtained in the absence and presence of oxygen, respectively, for the MeOH containing solution while (c–e) were obtained in the presence of oxygen for various alcohol-containing solutions; EtOH (c), *i*-PrOH (d) and *n*-PrOH (e). Since the reduced species has the absorption maximum at 420 nm, the increase of absorption at  $t=0$ , when the laser pulse at 355 nm with 10 ns duration was fired, indicates that photoreduction has occurred. It is apparent that the photoreduction takes place irrespective of the presence or absence of oxygen. In the presence of oxygen (b–e), however, it is reoxidized in 50 ms, while the reduced state lasts in its absence (a). The rate of oxidation depends on the  $\text{O}_2$  concentration. The individual curves shown in Fig. 7A(b–e) are well reproduced by a single exponential decay curve with an arbitrary time constant (the determined values are cited in the figure captions) as illustrated by thin solid lines in Fig. 7A. The curve displayed in Fig. 7(B) was observed for the

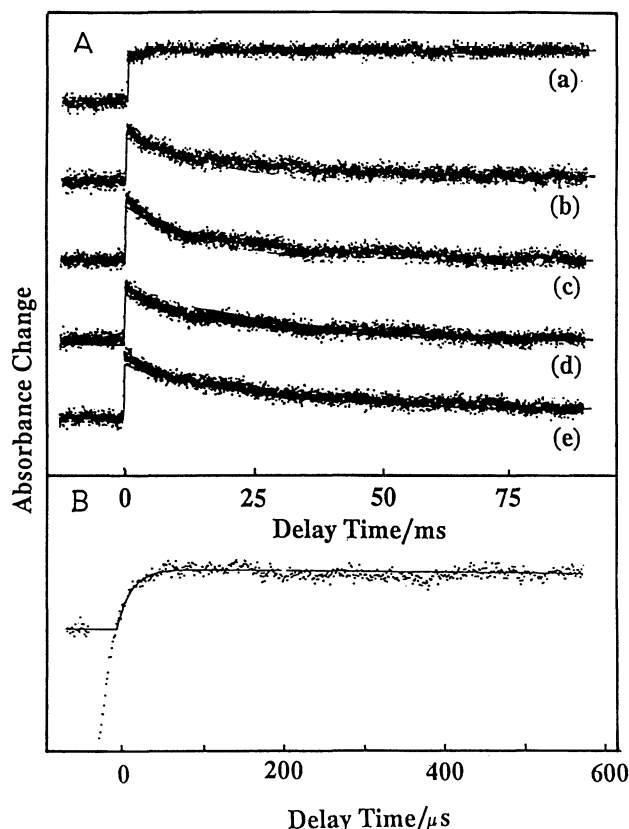


Fig. 7. Time profile of the absorbance at 420 nm after photolysis by the 355 nm pulse (10 ns width). A) (a)  $\text{Fe}^{\text{III}}(\text{OEP})(2\text{MeIm})(\text{MeOH})$  under anaerobic conditions, (b)  $\text{Fe}^{\text{III}}(\text{OEP})(2\text{MeIm})(\text{MeOH})$ , (c)  $\text{Fe}^{\text{III}}(\text{OEP})(2\text{MeIm})(\text{EtOH})$ , (d)  $\text{Fe}^{\text{III}}(\text{OEP})(2\text{MeIm})(n\text{-PrOH})$ , (e)  $\text{Fe}^{\text{III}}(\text{OEP})(2\text{MeIm})(i\text{-PrOH})$ . All spectra for (b)–e) were obtained under the same aerobic conditions. The thin solid lines were calculated by assuming the single exponential decay; the decay constants are 17.9 ms for MeOH, 16.5 ms for EtOH, 20.7 ms for *n*-PrOH, and 25.0 ms for *i*-PrOH under an atmospheric pressure. B) Time profile in the shorter delay time region of (A-a). The solid line indicates the calculated curve obtained by assuming that both the rise and decay are single exponential;  $\tau_{\text{rise}}=14.1 \mu\text{s}$  and  $\tau_{\text{decay}}=15.8 \text{ ms}$ .

MeOH containing solution on shorter time scale. The thin solid line was obtained by assuming that both the rise and decay are single exponential. This suggests that the photoreduction occurs with a time constant of 17  $\mu\text{s}$ . The apparently slow photoreaction implicates that it involves ligand replacement besides simple electron transfer.

### Discussion

The photoreduction described here has two characteristics; cooperative action of axial ligands and no photoreducibility under the CT excitation. When Im or 1-MeIm are present besides alcohol, it forms a bis-coordinate complex and alcohol cannot bind to the axial position due to its weak ligand field. Accord-

ingly, photoreduction does not occur. On the other hand, when  $\text{Fe}^{\text{III}}(\text{OEP})\text{Cl}$  is dissolved in  $\text{CH}_2\text{Cl}_2\text{--MeOH}$  mixed solvent, MeOH is considered to bind to the iron ion but photoreduction was not seen. Therefore, simultaneous coordinations of a N base and an alcohol are required for photoreduction to occur. The next question is what is an electron donor?

The primary and secondary alcohols were effective but a tertiary alcohol was not. One interpretation assumes a role of  $\text{C}_\alpha$ -hydrogen of alcohol, which occasionally serves as a reductant.<sup>10,33</sup> This would be likely if *t*-BuOH were bound to the sixth coordination position but photoreduction did not occur. Actually, however, *t*-BuOH gave neither the CT absorption band nor the Fe–alcohol stretching RR band, and therefore it is more reasonable to deduce that *t*-BuOH was not bound to the iron ion. The coordination of *t*-BuOH to the iron ion is probably inhibited by steric hindrance between  $\text{CH}_3$  hydrogen and pyrrole nitrogen. An alternative interpretation is to regard an N base as an electron donor as postulated in the previous study.<sup>17</sup> In order to determine the alternative we carried out gas chromatographic analysis of the photoreduced solution. The product was not a simple compound like formaldehyde and acetone. Unfortunately, however, we failed to identify the product by this analysis. The requirement is to prepare an enough of the product to determine its NMR spectrum.

Upon excitation of Raman scattering within the new absorption band around 590 nm, both the Fe–alcohol stretching RR band and the ordinary porphyrin bands characteristic for the Q band excitation<sup>26,27</sup> were observed. Therefore, the 585 nm absorption band should have a CT character besides the porphyrin  $\pi\pi^*$  character. The fact that the laser illumination in the 550–600 nm region did not induce photoreduction may imply alcohol is not an electron donor.

The Fe–2MeIm stretching RR band for  $\text{Fe}^{\text{II}}(\text{OEP})(2\text{MeIm})$  was observed at  $206 \text{ cm}^{-1}$  upon excitation at  $441.6 \text{ nm}$ <sup>17</sup>) but not upon red excitations. We failed to observe the  $\text{Fe}^{\text{III}}\text{--}2\text{MeIm}$  stretching RR band and therefore it is not clear where a CT band from 2MeIm to  $\text{Fe}^{\text{III}}$  is located. If it were present below 450 nm, the occurrence of photoreduction would be reasonably explained in terms of the CT excited state from 2MeIm to the  $\text{Fe}^{\text{III}}$  ion. Anyway, elucidation of photoreduction mechanism of iron porphyrin as well as heme proteins requires further study and the pump/probe time-resolved RR experiments for determining the structure of photoreduction intermediates are currently under investigation in this laboratory.

The authors thank Professor Y. Ozaki of Kwansai Gakuin Univ. for stimulating discussion and Dr. T. Ohta of chemical material center of this institute for the gas chromatographic analysis of solvents and products. V. F. is indebted to IMS for financial support during his stay in IMS at Okazaki.

## References

- 1) F. Adar and T. Yonetani, *Biochim. Biophys. Acta*, **502**, 80 (1978).
  - 2) I. Salmeen, L. Rimai, and G. T. Babcock, *Biochemistry*, **17**, 800 (1978).
  - 3) T. Kitagawa and Y. Orii, *J. Biochem. (Tokyo)*, **84**, 1245 (1978).
  - 4) T. Ogura, N. Sone, K. Tagawa, and T. Kitagawa, *Biochemistry*, **23**, 2826 (1984).
  - 5) T. Kitagawa and K. Nagai, *Nature (London)*, **281**, 503 (1979).
  - 6) T. Kitagawa, S. Chihara, K. Fushitani, and H. Morimoto, *J. Am. Chem. Soc.*, **106**, 1860 (1984).
  - 7) S. Yoshikawa, H. Mochizuki, S. Chihara, B. Hagihara, and T. Kitagawa, *Biochim. Biophys. Acta*, **786**, 267 (1984).
  - 8) J. T. Sage, D. Morikis, and P. M. Champion, *J. Chem. Phys.*, **90**, 3015 (1989).
  - 9) A. Harriman and G. Porter, *J. Chem. Soc., Faraday Trans.*, **75**, 1543 (1979).
  - 10) C. Bartocci, F. Scandola, A. Ferri, and V. Carassiti, *J. Am. Chem. Soc.*, **102**, 7067 (1980).
  - 11) C. Bartocci, A. Maldotti, O. Traverso, C. A. Bigozzi, and V. Carassiti, *Polyhedron*, **2**, 97 (1983).
  - 12) A. Maldotti, C. Bartocci, R. Amadelli, and V. Carassiti, *Inorg. Chim. Acta*, **74**, 275 (1983).
  - 13) C. Bizet, P. Morliere, D. Brault, O. Delgado, M. Bazin, and R. Santus, *Photochem. Photobiol.*, **34**, 315 (1981).
  - 14) M. Hoshino, S. Konishi, and M. Imamura, *Bull. Chem. Soc. Jpn.*, **57**, 1713 (1984).
  - 15) T. Imamura, T. Jin, T. Suzuki, and M. Fujimoto, *Chem. Lett.*, **1985**, 847.
  - 16) K. Kalyanasundaram, *J. Photochem. Photobiol., A Chem.*, **42**, 87 (1988).
  - 17) Y. Ozaki, K. Iriyama, H. Ogoshi, and T. Kitagawa, *J. Am. Chem. Soc.*, **109**, 5583 (1987).
  - 18) T. Ogura, V. Fidler, Y. Ozaki, and T. Kitagawa, *Chem. Phys. Lett.*, **169**, 457 (1990).
  - 19) V. Fidler, T. Ogura, S. Sato, and T. Kitagawa, in *Proceedings of the VIth Intl. Conf. on Energy and Electron Transfer*, Prague, **2**, 170 (1989).
  - 20) H. Ogoshi, E. Watanabe, Z. Yoshida, J. Kincaid, and K. Nakamoto, *J. Am. Chem. Soc.*, **95**, 2845 (1973).
  - 21) H. Ogoshi, H. Sugimoto, and Z. Yoshida, *Bull. Chem. Soc. Jpn.*, **54**, 3414 (1984).
  - 22) T. Ogura and T. Kitagawa, to be published.
  - 23) T. Kitagawa, M. Abe, and H. Ogoshi, *J. Chem. Phys.*, **69**, 4516 (1978).
  - 24) M. Abe, T. Kitagawa, and Y. Kyogoku, *J. Chem. Phys.*, **69**, 4526 (1978).
  - 25) X-Y. Li, R. S. Czernuszewicz, J. R. Kincaid, P. Stein, and T. G. Spiro, *J. Phys. Chem.*, **94**, 47 (1990).
  - 26) T. Kitagawa and Y. Ozaki, *Struct. Bonding*, **64**, 71 (1987).
  - 27) T. G. Spiro and X-Y. Li, in "Biological Application of Raman Spectroscopy," ed by T. G. Spiro, John Wiley & Sons, New York (1987), Vol. 3, Chap. 1.
  - 28) J. Teraoka and T. Kitagawa, *J. Phys. Chem.*, **84**, 1928 (1980).
  - 29) T. G. Spiro, J. D. Stong, and P. Stein, *J. Am. Chem. Soc.*, **101**, 2648 (1979).
  - 30) Y. Ozaki, K. Iriyama, H. Ogoshi, T. Ochiai, and T. Kitagawa, *J. Phys. Chem.*, **90**, 6105 (1986).
  - 31) T. Kitagawa, M. Abe, Y. Kyogoku, H. Ogoshi, H. Sugimoto, and Z. Yoshida, *Chem. Phys. Lett.*, **48**, 55 (1977).
  - 32) T. Kitagawa, H. Ogoshi, E. Watanabe, and Z. Yoshida, *Chem. Phys. Lett.*, **30**, 451 (1975).
  - 33) K. Hatano, K. Usui, and Y. Ishida, *Bull. Chem. Soc. Jpn.*, **54**, 413 (1981).
-